Role of Monovalent Counterions in the Ultrafast Dynamics of DNA

Sobhan Sen,[†] Latha A. Gearheart,[‡] Evan Rivers,[†] Hai Liu,[§] Robert S. Coleman,[§] Catherine J. Murphy,[†] and Mark A. Berg*[,†]

Department of Chemistry and Biochemistry, University of South Carolina, Columbia, South Carolina 29208, Department of Chemistry, Presbyterian College, Clinton, South Carolina 29325, and Department of Chemistry, The Ohio State University, Columbus, Ohio 43210

Received: November 2, 2005; In Final Form: May 5, 2006

This paper examines the contribution of counterion motion to the electric-field dynamics in the interior of DNA. The electric field is measured by a coumarin fluorophore that is synthetically incorporated into an oligonucleotide, where it replaces a native base pair. The DNA is a 17-base-pair oligomer with no A- or G-tracts. Time-resolved Stokes-shift measurements on the coumarin are made from 40 ps to 40 ns with each of the alkali ions and or one of several tetraalkylammonium ions as the DNA counterion. With the possible exception of rubidium, there are no indications of site-specific binding of the counterions. For sodium and other ions with a smaller hydrodynamic radius, the dynamics are identical and are fit to a power law. For larger ions, there is a progressive increase in the rate of shifting after 1 ns. This effect correlates with the hydrodynamic radius of the counterion. The lack of change in the spectral shape of the emission shows that neither the broadly distributed power-law relaxation nor the extra nanosecond dynamics are due to heterogeneity in the relaxation rates of different helices.

Introduction

DNA is a polyanion with one negatively charged phosphate group for every nucleobase. As a result, there are strong interactions between the DNA and its counterions in solution.[1] In isolation, the DNA charge is partially compensated by a "condensation" layer of counterions approximately 10 Å thick and containing 75% of the total DNA charge.[2,3] In complexes with proteins, the binding to and induced bending of DNA both depend critically on displacement of the counterions by charged protein residues.[4,5] Multivalent counterions can induce aggregation of DNA into complex forms.[6] Divalent counterions are hypothesized to cause localized bending of the DNA.[7] Monovalent ions can transiently bind in either the minor or the major groove of certain DNA sequences, notably A-tracts and G-tracts, although the extent and structural consequences of this binding remain controversial.[8]

Understanding any of these DNA−ion interactions would benefit from knowledge of the dynamics of the ions and the ions' affects on DNA motions. Most of these motions lie in the picosecond and nanosecond time ranges where few methods have been available for measuring DNA dynamics. In recent years, time-resolved Stokes-shift (TRSS) spectroscopy has been developed as a method of measuring the electric-field dynamics in DNA with time resolution down to the femtosecond level.[9−16] This method has the potential for measuring the interaction of DNA with its counterions directly on time scales of the ion motion. In this paper, we begin the systematic examination of these interactions by looking at the simplest case, a generic oligonucleotide sequence interacting with monovalent counterions.

CHART 1: Time-Resolved Stokes-Shift Probe (Coumarin-102 Opposed to Abasic Site) and the Native Base Pair It Replaces (Guanine Opposed to Cytosine)

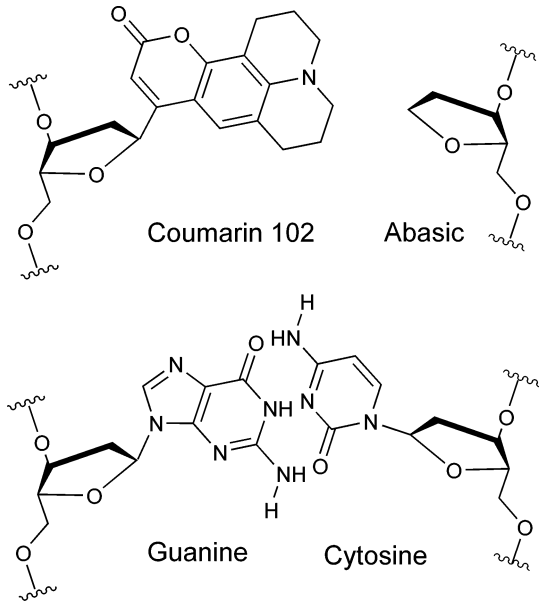

The TRSS experiments rely on an oligonucleotide in which a coumarin-102 system is substituted for one of the native base pairs (Chart 1). The coumarin group is covalently attached to the deoxyribose on one DNA strand; the opposing site on the complementary strand has an abasic site.[17] Positioned within the DNA base stack, the coumarin is placed to report on effects that are normally experienced by a DNA base. The DNA structure shows only modest changes due to this substitution and continues to be biologically active.[12] Although it is shielded from contact with the solvent,[12] the relatively long-range electrostatic field of the ions may still allow a direct interaction

* Author to whom correspondence should be addressed. Phone: (803) 777-1514. Fax: (803) 777-1456. E-mail: berg@mail.chem.sc.edu.
[†] University of South Carolina.
[‡] Presbyterian College.
[§] The Ohio State University.

10.1021/jp056327+ CCC: $33.50
Published on Web 06/14/2006

of the coumarin with the counterions. Alternatively, the counterions may alter the DNA's motion and thereby have an indirect affect on the coumarin.

Coumarin 102 is a solvatochromic dye; its absorption and emission spectra are sensitive to the electric field created at the dye by the local environment.[18,19] This sensitivity arises because coumarin's dipole moment is larger in the excited state than in the ground state. In the TRSS experiment, a short pulse of light initially creates the excited state and the associated increase in dipole moment $\Delta\mu$. Charged groups near the coumarin reorganize to solvate this new dipole. These groups include counterions as well as water and components of the DNA itself.[20]

The movement of the DNA and its local environment in response to $\Delta\mu$ causes the electric field at the coumarin to increase. The change in the electric field at the coumarin, the reaction field $\Delta\mathbf{E}$, stabilizes the excited-state dipole and causes the coumarin's emission spectrum to shift to lower frequency by an amount $\Delta\omega = -\Delta\mathbf{E}\cdot\Delta\mu$. The TRSS experiment consists of measuring the emission spectrum and the shift in its mean position, the Stokes shift, as a function of time after excitation.

The TRSS experiment is analogous to a dielectric-relaxation experiment, except that a dipolar field from a point source (the coumarin) is used in place of the uniform field from the macroscopic plates of a dielectric-relaxation experiment. The $\Delta\mu$ of the coumarin serves both to create a weak perturbing field in the DNA and to measure the reaction field created by the DNA in response to that perturbation. Thus, the Stokes shift is a direct reflection of the electric-field dynamics at the coumarin.

The TRSS experiment measures the electric-field dynamics of DNA in response to a small perturbation. However, by a linear-response argument, the time-dependent Stokes shift $S(t)$ following a weak perturbation is identical to the correlation function of the electric-field fluctuations at thermal equilibrium, i.e., in the absence of excitation of the coumarin

$$S(t) = \omega(\infty) - \omega(t) = \frac{1}{kT}\langle(\Delta\mathbf{E}(t)\cdot\Delta\mu)(\Delta\mathbf{E}(0)\cdot\Delta\mu)\rangle_{eq} \quad (1)$$

This relationship has been confirmed in a recent computer simulation.[20] Both the magnitude and the time dependence of the nonequilibrium Stokes shift from experiment match the equilibrium electric-field correlation function from simulation, as predicted by eq 1. Thus, the coumarin serves as a passive probe in the TRSS experiment. It measures the unperturbed thermal motions of its immediate surroundings. In this fashion, TRSS measurements give a window on the local motions occurring in DNA on short time scales.

DNA motions must affect the electric field to be measured by TRSS. Such motions are analogous to the motions that cause solvation dynamics and polarity in simple solutions. Both solvation dynamics and polarity directly affect the rate of chemical reactions that involve charge transfer, either in the product or in the transition state.[21] Thus TRSS measurements not only provide a general sampling of DNA dynamics, they specifically sample motions likely to play a role in chemical reactions occurring within DNA.

In DNA, the dynamics monitored by TRSS extend over at least six decades in time.[13,14] Over this entire range, the results can be fit to a power law. Particularly interesting is the fact that these dynamics extend to very long times. For example, the corresponding solvation dynamics in water are complete in 1−2 ps,[14,22] but the dynamics in DNA are not equilibrated at 40 ns, the longest time measured.[10,13,14]

Neither the origin of the power-law form of the dynamics nor the reason that they continue to such long times has been explained. However, counterion dynamics are a primary suspect. Computer simulations have shown that convergence of the ion configurations can require many nanoseconds.[23,24] The TRSS response in electrolyte solutions has slow, nanosecond components due to ion diffusion,[25] although it does not develop the extended, power-law relaxation characteristic of DNA.

In this paper, we look at the effect of changing the DNA counterion on the TRSS experiment in the hopes of identifying counterion contributions to the dynamics. The existing evidence on differences between monovalent DNA counterions is incomplete. NMR experiments measure ion affinities for DNA by monitoring the displacement of Na^+. These experiments do not find strong differences between the alkali ions, although they do find that large alkylammonium ions have a weaker affinity for DNA.[26,27] Counterion-specific binding has been seen in more recent NMR experiments but only for special sequences (A-tracts).[28,29] Computer simulations have begun to provided a detailed picture of ion distributions and motions,[30,31] but only a few reports have explicitly compared different counterions: Lyubarsev and Laaksonen have compared Li^+, Na^+, and Cs^+;[32] Várnai and Zakzewska have compared Na^+ to K^+.[23] Despite the similar behavior of the alkali ions in NMR experiments, the computer simulations find significant differences in the spatial distribution of different counterions around DNA.

This paper presents TRSS results for DNA with counterions with a variety of sizes, each of the alkali ions (Li^+, Na^+, K^+, Rb^+, and Cs^+) and a series of tetraalkylammonium ions (NH_4^+, $N(CH_3)_4^+$, $N(C_2H_5)_4^+$, and $N(C_4H_9)_4^+$). We expected to see either a smooth change with size—for example, a slowing of the TRSS response with larger ions due to slowing of the ion diffusion—or unusual behavior with ions of a specific size, an effect which would indicate the existence of size-specific binding sites on the DNA. These effects were not seen. Instead, the smaller counterions give identical results, while the larger ions have an unexpected increase in the rate of Stokes shifting at long times. This latter effect correlates with the hydrodynamic radius of the counterion.

Because the final effects are of modest size, the reproducibility and error limits in the TRSS technique are characterized in detail before presenting the main results. We also test the hypothesis that the broadly distributed TRSS relaxation is due to a distribution of relaxation times among different helices within the sample. Such heterogeneous dynamics would result in time-dependent shapes of the emission spectra. These shape changes are not found, and we conclude that heterogeneous dynamics are not the reason that the electric-field dynamics extend over such a broad range of times.

Materials and Methods

Sample Preparation. The oligodeoxynucleotide 5′-GCAT-GCGC(cou)CGCGTACG-3′ containing coumarin-102 C-deoxyriboside (cou) was synthesized as described earlier.[9,17] The complementary strand containing an abasic-site analog[33] opposite the coumarin was obtained commercially. Both oligonucleotides were initially dissolved as concentrated solutions in sodium phosphate buffer. Double-stranded helices with sodium counterions were made directly by diluting and annealing the two strands to a final concentration of 25 μM (duplex) in 100 mM pH 7.2 sodium phosphate buffer. DNA concentrations were measured by the absorbance at 260 nm, using the sum of extinction coefficients for individual bases.

Samples with other counterions were made by ion exchange of the individual single strands. Dry Sephadex-CM C-50 resin

was hydrated with deionized water for 2 days. A 4-cm-long, 10-mm-diameter column of the resin was charged by running a 1 M hydroxide solution of the corresponding cation through the column. The column was washed with pure water and then with 10−30 mM phosphate buffer (pH 7.2) of the desired cation. (Because lithium phosphate is insoluble, cacodylate ion AsO_4^{3-} was substituted for phosphate in all lithium-containing solutions.) An aliquot of concentrated (∼100 μM duplex) oligonucleotide solution (6 nmol typical) was eluted through the column with additional phosphate buffer. The DNA-containing fraction was collected, concentrated, and rediluted to a final buffer concentration of 100 mM. Annealing complementary strands produced final DNA concentrations of 20−30 μM (duplex).

This procedure left less than 0.01 ppm of the original Na^+ ions in the final DNA solutions as judged by atomic absorption analyses of the final solutions (Robertson Microlit Laboratories). Several samples were prepared and measured multiple times to check the reproducibility of the sample preparation and the TRSS measurement: Na^+, NH_4^+, and Rb^+ three times each and Li^+ twice. No systematic variations were found. The reported results are the average of all independent measurements with the same counterion.

Steady-State Spectroscopy. Steady-state excitation and emission spectra were collected using magic-angle polarization (54.7°). Emission spectra were excited at 390 nm; excitation spectra were detected at 500 nm. The native DNA bases are essentially nonfluorescent,[34] so only the coumarin contributes to these spectra. Frequency band-passes were 4 nm in all cases. The silica sample cells were silanized to reduce scattered light from DNA adsorbed to the cell walls. The raw emission spectra were corrected for instrumental sensitivity by using a correction factor obtained from a quinine-sulfate standard.[35] It was found that obtaining quantitatively reproducible results required measuring the standard within a few days of and in the same cell as the sample measurement.

All spectra were converted to susceptibility χ versus frequency ν before analysis. This presentation corrects for trivial frequency factors that occur in the expressions for the absorption spectrum A and emission intensity $I(\lambda)$,[11] specifically

$$\chi(\nu) = A(\nu)/\nu; \quad \chi(\nu) = I_p(\nu)/\nu^3; \quad I_p(\nu) = I(\lambda)/\nu^3$$

where $I(\lambda)$ is in radiometric units (W/nm).[36] Susceptibility spectra from absorption and emission can be compared directly; they are mirror images under standard assumptions. Spectra on a frequency axis shift linearly with energy relaxation of the solute; spectra on a wavelength axis shift nonlinearly. Thus, failure to use a susceptibility versus frequency representation introduces small, but unnecessary, errors into the TRSS measurements.

Spectra in a rigid glassy matrix were measured by adding glycerol to the samples to make a 1:3 mixture of buffer and glycerol. The samples were then frozen in a dry ice/acetone bath (190 K) before collecting the spectra.

Time-Resolved Spectroscopy. Time-resolved emission spectra were measured using time-correlated single-photon counting (TCSPC).[37,38] Approximately 100 fs pulses from a mode-locked Ti:sapphire laser were frequency doubled to 390 nm in a 1 mm β-barium borate (BBO) crystal. The 80 MHz repetition rate of the laser was reduced to 6 MHz by an acousto-optic pulse selector. The samples were excited by 4 mW of light focused through the bottom of a 1 mm × 1 mm silanized cuvette with the beam parallel to the monochromator slits. The samples were held at 15 °C to ensure complete hybridization of the DNA.

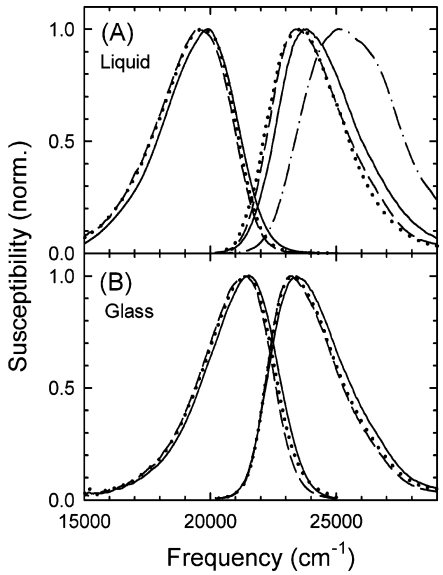

Figure 1. Examples of fluorescence excitation (right) and emission (left) spectra of coumarin-containing DNA in the presence of $N(C_4H_9)_4^+$ (solid), Na^+ (dashed), and Cs^+ (dotted) either (A) in room-temperature aqueous solution or (B) in a rigid glass. The excitation spectrum of coumarin 102 in water (dash−dotted) is shown in part A for comparison.[9] Shifts between different ions are small (Table 1). The spectra are plotted in susceptibility vs frequency. In this format, excitation and emission spectra are expected to show mirror symmetry.

Fluorescence from a 10 mm length of the excitation beam was collected at right angles to the beam and passed through a Glan-laser polarizer at the magic angle (54.7°) to the excitation polarization. The fluorescence passed through a 2 nm band-pass and 0.22 m single monochromator before detection on a microchannel plate and timing by standard TCSPC counting electronics. The typical instrument response of the system was 45 ps full width at half maximum (fwhm) as measured by scattering from a silica suspension in water.

Sample degradation was checked for by comparing the steady-state spectra before and after data collection. With a 40 μL sample volume (20−30 μM duplex) exposed to 4 mW of excitation laser power for 4−6 h, degradation was negligible. A total of 3×10^7 counts were collected at each wavelength, except the two most extreme wavelengths, where a total of 1×10^7 counts were collected.

Data collection and analysis followed standard methods.[18] Fluorescence decays were collected at 16 different wavelengths (11 for Na^+) ranging from 415 to 640 nm. The decays were fit to a sum of 3−5 exponentials by iterative reconvolution with the instrument response function. The relative amplitudes at each wavelength were scaled so that the integrated intensity under each decay matched the steady-state emission amplitude at that wavelength. The emission spectrum at any time can be read from these scaled fits. Because the steady-state emission spectra used to scale the data are in the form of susceptibility versus frequency, the time-resolved emission spectra are also in the form of susceptibility versus frequency. The measured frequency points in the time-resolved spectra were interpolated, and the mean spectral positions were characterized as the first moments, as described before.[11]

Results

Steady-State Spectra with Different Counterions. The place to begin looking for possible differences between counterions is in the steady-state excitation spectra. Figure 1A shows excitation spectra of coumarin in DNA in the presence of three

TABLE 1: Positions of the Steady-State Spectra of Coumarin in DNA with Various Counterions[a]

	liquid		glass	
counterion	absorption shift (cm^{-1})	apparent Stokes shift (cm^{-1})	absorption shift (cm^{-1})	apparent Stokes shift (cm^{-1})
$N(C_4H_9)_4^+$	760	5820	190	3480
$N(C_2H_5)_4^+$	130	5370	160	3530
$N(CH_3)_4^+$	270	5480	210	3530
NH_4^+	200	5500	180	3600
Li^+	−10	5200	240	3650
Na^+	0	5360	0	3530
K^+	−80	5220	120	3590
Rb^+	290	5580	230	3590
Cs^+	−70	5230	90	3510
coumarin in water[b]	1780	6790		

[a] Absorption shifts are given as the first moments of the excitation spectra relative to sodium. The apparent Stokes shift is the difference between the first moments of the excitation and steady-state emission spectra. The absolute positions for sodium are 24 320 cm^{-1} (liquid absorption) and 24 140 cm^{-1} (glass absorption). See Figures 1 and 7. [b] Reference 9.

representative counterions: Na^+, Cs^+, and $N(C_4H_9)_4^+$. The excitation spectra with the other counterions, Li^+, K^+, NH_4^+, $N(CH_3)_4^+$ and $N(C_2H_5)_4^+$, are similar and fall within the same range of shifts. For comparison, the spectrum of coumarin 102 free in water is also shown. The relative shifts of the excitation spectra between the ions are listed in Table 1.

As discussed previously,[9] the environmentally sensitive absorption spectrum of coumarin shifts substantially when it is embedded in DNA rather than free in water. In comparison to this large change, the shifts among DNA samples with different counterions are quite small. No clear pattern in these shifts emerges, except that the alkylammonium-ion spectra are shifted to slightly higher frequencies.

The small shifts could result from some change in the average spatial distribution of different ions, an effect that has been seen in computer simulations. Overall, there is not any indication in the absorption spectra of a significant change in the static structure as the counterion is varied.

Figure 1A also shows the emission spectra of coumarin-containing DNA in the presence of the same three counterions. The large shifts between the emission and the excitation spectra (Stokes shift) indicate that there has been substantial relaxation of the environment around coumarin in its excited state. This shift has been discussed previously.[10−14,20] The apparent Stokes shifts, defined here as the difference between the first moments of the absorption and emission spectra, are given in Table 1. Again, there are only small differences upon changing the counterion; all the Stokes shifts lie within a 300 cm^{-1} range except for Rb^+ and $N(C_4H_9)_4^+$. The TRSS data discussed below are more sensitive to differences in the samples than these steady-state measurements. However, we anticipate that the differences will be small, and thus we examine the error limits of TRSS in detail in the next section.

Figure 1B shows examples of spectra of the coumarin-containing DNA in a frozen, glassy matrix. Despite the rigidity of the matrix, the apparent Stokes shift (measured between the peaks of the absorption and emission spectra) is not zero (Table 1). This Stokes shift is due in part to the unresolved vibronic structure of the absorption and emission spectra. Even if the Stokes shift measured between the 0−0 transitions of each spectrum were zero, there would be an apparent Stokes shift between the peaks of the vibronic structure. This effect is not of interest, because it is an intramolecular property of the coumarin, not a property of the DNA.

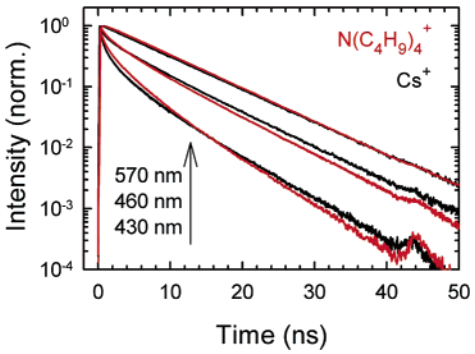

Figure 2. Examples of wavelength-resolved fluorescence decays of coumarin-containing DNA in the presence of Cs^+ (black) and $N(C_4H_9)_4^+$ (red) at three different wavelengths (430, 460, and 570 nm, bottom to top). The changes between different wavelengths indicate the presence of a time-dependent Stokes shift. The differences between the Cs^+ and the $N(C_4H_9)_4^+$ transients show the ion dependence of the time-dependent Stokes shift.

In addition, there is a small Stokes shift due to relaxation of the coumarin environment, even in the frozen glass. This relaxation is due to the emission of phonons into the solid matrix. When the matrix melts, these phonon motions evolve into the inertial component of dynamics in a liquid.[39,40] The relaxation of these motions is very rapid (<50 fs), whether in the glass or a liquid solution. The dynamics of this relaxation can be understood from a normal-mode analysis of the instantaneous structure of the DNA and surrounding solvent.[41]

Here we focus on the relatively slow diffusive (nonvibrational) relaxations that are present in the fluid but not in the glass. We define an absolute Stokes shift as the difference in the first moments of the emission spectrum in the fluid and in the glass. This definition assumes that the spectral shifts due to adding the cryogen (glycerol) to the solution and due to the low temperature of the glass (190 K) are negligible. Measurements with high time resolution indicate that the emission spectrum in the room-temperature fluid extrapolates at zero time to the position of the glass spectrum to within 200 cm^{-1}.[13,14] This absolute Stokes-shift scale can be used to infer the amount of Stokes shifting caused by dynamics faster than our time resolution. However, these inferred values will not be as accurate as the directly measured Stokes shifts within our measured time window.

Reproducibility of TRSS Measurements. Figure 2 shows examples of raw fluorescence intensity transients of coumarin-containing DNA at three different wavelengths for two different counterions. Note that the high sensitivity of time-correlated single-photon counting allows the fluorescence decays, and thus the Stokes shifts, to be measured out to seven lifetimes or more. The transients clearly show measurable differences between ions at these long times. However, there is clearly a concern as to how far out in time the Stokes-shift measurements can be made before the noise in the fluorescence decays creates an unacceptable level of uncertainty.

In many experiments, the random scatter of the data points is a good indicator of the experimental error, but not in the current experiments. In the data analysis, the fluorescence transients are fit to an analytical form before further analysis. This procedure removes the random scatter of the data and introduces strong correlations between the final data points. In addition, there are many sources of potential systematic errors: deconvolution of the instrument response function, interference

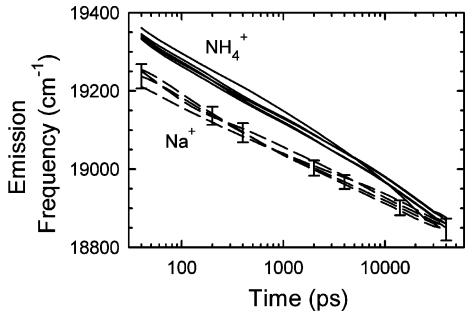

Figure 3. Comparison of repeated measurements of the time-resolved emission frequency of coumarin-containing DNA with Na^+ (dashed lines) and NH_4^+ (solid lines) counterions. The error bars (shown on the Na^+ data) are plus and minus two standard deviations. The errors are less than the differences between the two ions.

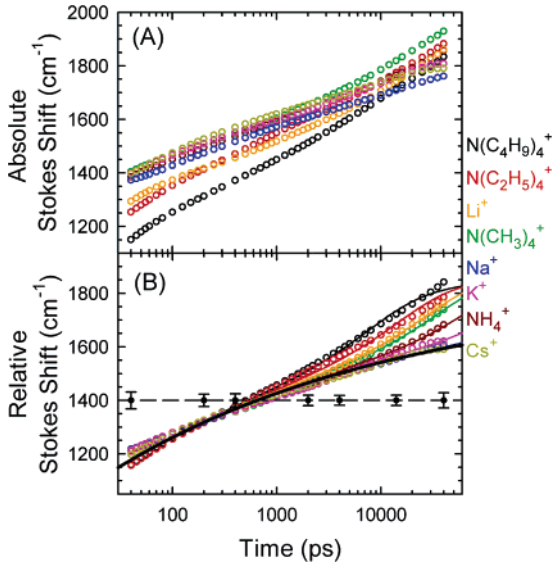

Figure 4. Time-resolved Stokes shifts in DNA with different counterions. (A) Absolute Stokes shifts of DNA in the presence of eight different counterions relative to the corresponding steady-state glass emission spectra. (B) Stokes shifts shifted vertically to match the Cs^+ results at early times. The solid curves are fits to the TRSS data (points) with an unvarying power law plus an ion-dependent exponential relaxation (eq 3). The power-law component is plotted as a thick black solid curve. The error bars at different times (Figure 3) are plotted parallel to the time axis.

from scattered excitation light, the measurement of the steady-state emission spectrum, the extraction of the mean frequency of the spectrum, and the preparation of the sample.

We have chosen to characterize the reproducibility of TRSS experiments by replicating the entire measurement several times for two samples, Na^+ and NH_4^+ (Figure 3). These data sets include replicated samples, including different runs of the NH_4^+ exchange, different measurements of the steady-state spectrum, and different measurements of the fluorescence decays. The TRSS data for two of the Na^+ samples were taken by different people several years before the current measurements.[9,11]

The final error limits are calculated from the variations within both the Na^+ and the NH_4^+ data sets. Figure 3 shows the error as plus and minus two standard deviations at various time points on the Na^+ data. Over the time range presented (40 ps to 40 ns), the error is relatively constant. Outside this range, the error increases rapidly. Attempts to extract data at shorter times run into increased error due to the need to deconvolve the instrument response function (45 ps fwhm). At times longer than 40 ns, the loss of fluorescence intensity results in rapidly increasing errors (Figure 2). Fortunately, the measurements within the 40 ps to 40 ns time range are sufficiently reliable to detect the small differences between different counterions (Figure 3).

Time-Resolved Stokes-Shift Dynamics with Different Counterions. Time-resolved Stokes-shift experiments were carried out with nine different counterions. The results with rubidium, which are slightly anomalous, are discussed later. The results from the other counterions are shown in Figure 4. None of the data sets converges to an equilibrium value by the end of the measured time range (40 ns). This result has been seen in previous measurements.[10−14]

In Figure 4A, the shift of the emission is given relative to the emission spectrum in the corresponding glass. The shifts at the earliest measured time (40 ps) are already substantial, ranging from 1175 to 1400 cm^{-1}. This shift is due to dynamics that occur at even earlier times.[13] These shifts do appear to change somewhat with the counterion. However, these changes are not large compared to potential uncertainties in the absolute Stokes-shift scale. Thus, it is difficult to draw conclusions beyond the fact that differences in the early dynamics may exist. For similar reasons, it is difficult to judge whether there are systematic changes in the final absolute Stokes shift among the different ions.

In Figure 4B, the results have been shifted vertically to overlap with the Cs^+ data before 1 ns. This representation focuses on differences within the experimental time window, which are measured more accurately than the absolute Stokes shifts. The error bars measured in the previous section (Figure 3) are reproduced in this figure. A pattern in the ion-dependent behavior emerges in this presentation. Several ions, Cs^+, NH_4^+, K^+, and Na^+, have nearly identical TRSS curves over the entire time range. Previous measurements on Na^+ extending over a full six decades in time fit well to a simple power law[13,14]

$$S(t) = S_\infty\left[1 - \left(\frac{t}{t_0}\right)^{-\alpha}\right] \qquad (2)$$

This form has been fit to the Cs^+ data ($\alpha = 0.155$, $S_\infty = 2010$ cm^{-1}, $t_0 = 25$ fs) and is shown as the thick black curve in Figure 4B. In the sub-nanosecond region, the TRSS data of all ions are experimentally indistinguishable from each other or from the power law. At times longer than 1 ns, some ions continue to follow the power law, whereas others (Li^+ and the tetraalkylammonium ions) show varying degrees of deviation from the power law.

The magnitude of the deviation correlates with the hydrodynamic radius of the ions. The ions are listed in order of hydrodynamic radius on the right side of Figure 4. The hydrodynamic radius is derived from conductivity measurements[42] and includes the averaged effect of water bound to the ion tightly enough to affect its mobility. Thus, Li^+, which binds four waters very tightly, has a larger hydrodynamic radius than Cs^+, which binds water weakly. The expected effect of the ionic radius is an overall slowing of the Stokes shifting with larger ions. The observed effect, in which a new relaxation component appears for larger ions, is unexpected and is one of the major results of the paper.

To quantify this new effect, we used the following equation to fit all the data

$$S(t) = S_\infty\left[1 - \left(\frac{t}{t_0}\right)^{-\alpha}\right] + A[1 - e^{-kt}] + B \qquad (3)$$

In addition to the power-law term of eq 2, we have added an exponential relaxation with rate constant k and amplitude A. The constant B accounts for the shift used to match the TRSS

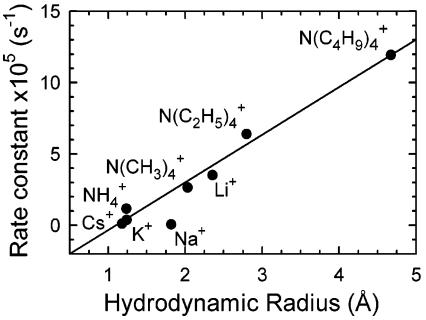

Figure 5. Variation of the rate constant k in eq 3 with the hydrodynamic radius of the counterion.

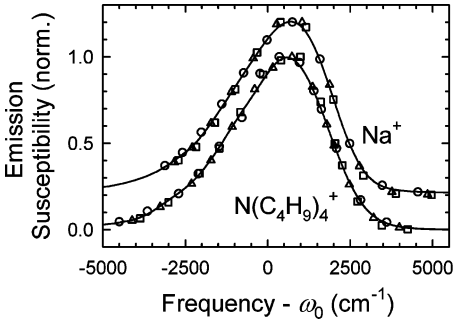

Figure 6. Time evolution of the shape of the emission spectrum. Spectra from different times have been shifted in frequency by their first moment ω_1 and normalized to 1 at the peak susceptibility to facilitate comparison of the shapes. Selected results from Na^+ and $N(C_4H_9)_4^+$ are shown: 40 ps (○), 4 ns (△), 40 ns (□). The main portion of the spectrum does not change shape with time, showing that dynamic heterogeneity is not important. See Supporting Information for more details.

data of each ion with the Cs^+ data at short times. The constants α, S_∞, and t_0 were fixed at the value used in the fit to the Cs^+ data to eq 2. The constant $A = 220$ cm^{-1} was determined by fitting the $N(C_4H_9)_4^+$ data. Only k and B were varied between different ions. The fits to the data are shown as solid curves in Figure 4B, and the fitting parameters are tabulated in the Supporting Information.

Figure 5 shows the rate constant k from eq 3 plotted against the hydrodynamic radius of the counterion. There is a clear correlation between these two quantities. Sodium appears to be an outlier from this correlation and is not included in the fit.

Although eq 3 is presented as an empirical characterization of the differences between TRSS traces with different ions, the equation necessarily implies assumptions about the nature of these differences. The picture implied by eq 3 is that there is a power-law relaxation at early times that switches over to an exponential relaxation at later times. The exponential relaxation is slow in the small ions and lies beyond the measurement window (>40 ns). However, the rate increases with ionic size, and the relaxation moves into the measurement time window for the large ions.

At present, it is not clear what physical mechanism should be associated with the exponential relaxation. However, there is an expectation that power-law relaxation may not continue indefinitely. Any nonexponential relaxation, including a power law, requires the system to maintain some type of memory of its initial structural fluctuation over the period of the relaxation, although this memory may not be in the observed coordinate.[43] In a finite system (e.g., a finite length oligomer), there will be some slowest relaxing coordinate that sets a maximum memory time. After the relaxation of this mode is complete, the TRSS relaxation would switch to exponential relaxation. Thus, one interpretation of eq 3 is that it represents the switch from power-law to exponential relaxation.

However, this fit and this interpretation are not unique. For example, it is also possible to keep k constant in eq 3 and vary the amplitude of the relaxation A. The quality of the fits is acceptable with this alternative fit. The trend of A with counterion mimics the trend of k when k is varied. Thus, Figure 5 shows that there is a correlation between the ion-dependent relaxation and the ion radius, but various mechanisms and fitting equations can be postulated to describe this correlation.

Dynamic Heterogeneity in Ion Configurations. The standard theory for time-resolved Stokes shifts predicts that the emission spectrum will shift in frequency without changing shape.[44] One possible exception to this result occurs when there is dynamic heterogeneity, in other words, when some molecules in the sample relax at a different rate than other molecules.[45]

In the current experiments, it is easy to hypothesize that individual DNA chains exist in different long-lived configurations (e.g., ion-bound and unbound) and that these configurations have intrinsically different rates of Stokes shifting. The superposition of fast and slow decays could account for the strongly nonexponential relaxation observed in experiments.

When dynamic heterogeneity is present, each subensemble of molecules may have the same initial emission spectrum and the same relaxed emission spectrum. However, if the different subensembles relax at different rates, then the spectrum of each subensemble will have a different frequency shift at intermediate times. As a result, the observed spectrum, which is the sum of the spectra of all the subensembles, will be broad. Thus dynamic heterogeneity leads to a characteristic broadening of the emission spectrum during the first half of the relaxation followed by narrowing during the second half. The current experiments only look at the second half of the relaxation, as judged by comparing the earliest measured absolute Stokes shift (Figure 4A) to the extrapolated final value. As a result, only a narrowing with time is expected in our measurements.

Figure 6 is constructed to emphasize any change in the shape of the emission spectra with time. Time-resolved emission spectra at three different times spanning the measurement range have been shifted horizontally by their mean frequencies ω_1 and normalized to the same peak amplitude. Spectra are shown with two different counterions, Na^+, which has the simple power-law relaxation that is characteristic of small ions, and $N(C_4H_9)_4^+$, which has the strongest long-time component that is associated with large counterions. However, Figure 6 shows that for each of the ions data points from different times match to a common spectral shape.

The maximum amount of broadening possible in the presence of strong dynamic heterogeneity is equal to the total Stokes shift. Considering the accuracy of the data, any broadening at the half-width of the spectra must be less than approximately 300 cm^{-1}, or less than 15% of the total range of the Stokes shift. Thus, heterogeneous dynamics are not important in this system and are not the explanation of the broad distribution of time scales in the relaxation.

In a previous publication, we reported an inaccurate measurement of the emission line-shape change with sodium as the counterion.[46] That error resulted from a small change in the shape of the blue tail of the emission spectrum that is not visible in Figure 6. This small tail is not sufficient to change the conclusions presented here, but for completeness, it is documented in the Supporting Information. In particular, there is no evidence for sodium-ion binding in the corrected measurements.

Anomalous Behavior of Rubidium. The results with Rb^+ as the DNA counterion differ perceptibly from those with other

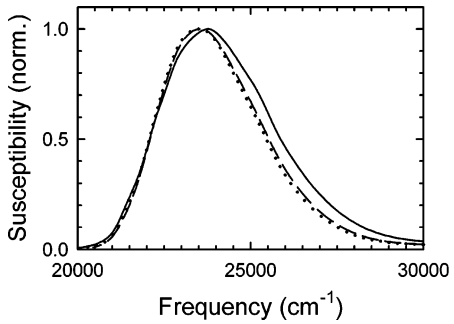

Figure 7. Room-temperature excitation spectra of coumarin-containing DNA with Rb^+ (solid), Cs^+ (dashed), and K^+ (dotted) counterions. The Rb^+ spectrum is the average of measurements on three independently prepared DNA samples. Its spectrum is consistently broader than the spectrum of any other ion.

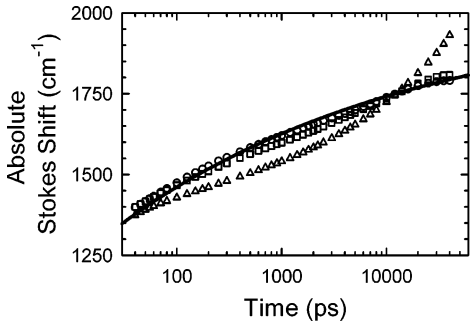

Figure 8. Comparison of the time-resolved Stokes shift of coumarin-containing DNA with Rb^+ (△), Cs^+ (○), and K^+ (□) counterions. The fit to eq 2 (also shown in Figure 4B) has been included as a solid black curve. The Rb^+ data differ from those of its neighbors in the periodic table.

ions. The change in the mean frequency of the spectrum, already listed in Table 1, only partly reveals this difference. More detail can be seen in Figure 7, which compares the excitation spectrum with Rb^+ to spectra with Cs^+ and K^+, rubidium's nearest neighbors in its column in the periodic table. Cesium and potassium give nearly identical spectra with fwhm's of 3400 cm^{-1}. Other ions give very similar widths. The spectrum with Rb^+ has a fwhm of 3760 cm^{-1}, noticeably broader than the spectra with any other ion. This difference is reproducible upon repeated measurements and independently ion-exchanged samples. In comparison to Cs^+ and K^+, the low-frequency side of the spectrum is unchanged with Rb^+; the broadening and shift in mean frequency are due to an increase in intensity on the high-frequency side of the spectrum.

The anomalous behavior of Rb^+ is also seen in the TRSS measurement. Figure 8 compares the TRSS results in the presence of Rb^+, Cs^+, and K^+ counterions. The fit to eq 2 is also shown as a black solid curve. The Rb^+ data are quite unlike the data with Cs^+ and K^+. The large Stokes shift after 1 ns does not match the correlation with hydrodynamic radius shown in Figure 5. The Stokes shift before 1 ns does not match well to a power law, and as a result, the rubidium data do not fit well to eq 3. Overall, the rubidium data do not match the trends seen with the other ions.

One explanation could be the existence of a binding site specific for Rb^+. For example, there could be a site in one of the grooves whose size fits Rb^+ better than any other ion. An equilibrium mixture of bound and unbound forms could account for the broadening of the excitation spectrum. In the TRSS experiment, the binding and unbinding kinetics would be superimposed on the dynamics seen with the other ions.

Other experiments offer little to either support or refute this proposal. Rubidium was not studied in the classic NMR experiments on monovalent cation binding.[26,27,47] More recent NMR[28] and X-ray[48] experiments on Rb^+ binding are specific to binding in A-tracts.

Even if an ion-specific binding site is being observed, it might be induced by the nonnative probe chromophore. Thus, the results presented here are at most equivocal evidence for a native Rb^+-specific binding site. The more useful conclusion lies in the converse. With the possible exception of Rb^+, none of the monovalent ions shows evidence of ion-specific interaction with DNA, in either the native or the probe-modified regions of the DNA.

Discussion and Conclusions

At the outset of this study, it was unclear whether monovalent counterions had the ability to strongly affect the electric field, effective polarity, or solvation dynamics in the interior of DNA. In pure water, as much as 85% of the solvation energy is due to molecules in the first solvation shell of the solute, a distance of only 5 Å.[49] Thus, it was conceivable that the interior of DNA could be effectively shielded from the influence of counterions. However, the existence of a large ion-dependent component to the results presented here allows us to conclude that counterion dynamics do affect the interior of DNA.

This conclusion is consistent with recent computer simulations that we analyzed in collaboration with the Beveridge group. That study shows that the electric field in the interior of DNA is affected by material out to a distance of approximately 15 Å from the probe chromophore, a volume large enough to contain significant amounts of both water and counterions.[20]

These simulations also indicate that the motion of the DNA itself contributes significantly to the electric-field dynamics measured in these experiments. It is also known that counterion concentration and valence affect the persistence length of the DNA.[5,50,51] Thus, it is possible that the effects measured here are indirect effects of the ions on the DNA motion rather than a direct effect of the ion motion itself.

Given that ions affect the electric-field dynamics in the interior of DNA, it is generally expected that the differences between monovalent counterions would be small. This expectation is supported by the current experiments for the small, commonly used counterions: Na^+, K^+, NH_4^+ and Cs^+. Their TRSS decays are indistinguishable.

The unexpected result from this study is the discovery of an extra relaxation after 1 ns in the larger ions: Li^+ and tetramethyl-, tetraethyl- and tetrabutylammonium. The size of this extra relaxation increases with the hydrodynamic radius of the ion. At present, it is not clear if this extra response is entirely absent in the smaller ions or if it takes place at longer times outside the measurement range.

NMR experiments distinguish two general types of Na^+ counterions: associated with the DNA and not associated. Titration with other counterions leads to a measure of the relative association constants for different ions with DNA. Interestingly, binding affinity correlates with hydrodynamic radius,[47] just as the extra TRSS feature does.

One possible cause for the extra relaxation is steric crowding of the ions. In computer simulations, local ion concentrations as high as 2−4 M are seen for small ions near the DNA surface,[32] corresponding to a volume per ion of 0.5−0.25 M^{-1}. For the largest ion in this study, $N(C_4H_9)_4^+$, the molar volume is 0.26 M^{-1}. Clearly crowding of the ions becomes a significant issue. This steric crowding may induce additional correlations in the ion motion that are not present for smaller ions.

Another possible contribution to the long-time dynamics of the large ions is the internal dynamics of the ions. The largest ions, $N(C_4H_9)_4^+$ and $N(C_2H_5)_4^+$, have considerable internal structure. The reorganization of the alkyl chains could affect the rate that the ion is able to move into positions close to the DNA. However, the $N(CH_3)_4^+$ ion does not have similar internal dynamics but does still show the extra dynamical component seen in the other ions. Thus, the hypothesis that the extra dynamics are due to internal ion reorganization is not entirely satisfactory.

Another concern in any study of DNA−ion interaction is the possibility of ion binding. Many types of ion binding have been considered in the literature: in the major groove, in the minor groove, at a phosphate, or bridging two phosphates. Because TRSS is sensitive to electric fields, most types of ion binding would create a signature in the TRSS response, and because a large range of ion sizes were studied, some modulation of binding ability is expected.

This study is most sensitive to size-specific binding sites. The existence of such sites would be signaled by anomalous behavior of the one or two ions with the correct size for binding in comparison to the general trends with ion size. There is no evidence for this type of binding for most of the ions. The possible exception is Rb^+, which has some weak but discernible anomalies. The lack of strong specific binding is not surprising, because the oligonucleotide studied does not have any of the sequence features that have been suggested to create good ion-binding sites.[8]

Ion-bound configurations have been hypothesized to gate electron transfer in DNA, because they would modify the hole states,[52] presumably due to an especially strong electric field in the DNA in the ion-bound configuration. Our experiments have not found evidence for such ion-bound configurations or other high-electric-field configurations that could serve to gate charge transfer in DNA.

In summary, this study has characterized the electric-field dynamics in a generic DNA sequence with monovalent counterions of various sizes. Small ions (Cs^+, NH_4^+, K^+, and Na^+) create indistinguishable dynamics. However, an unexpected additional relaxation component in the nanosecond time range occurs with larger counterions (Li^+ and the tetraalkylammonium ions). Ion binding is weak or nonexistent. These results form a baseline for future studies of more complex systems, including sequences believed to favor ion binding or systems with multivalent counterions, which interact more strongly with DNA.

Acknowledgment. This work was supported by the National Institutes of Health (Grant No. GM-61292).

Supporting Information Available: Additional detail on time-dependent changes in the emission line shape and tabulated fitting parameters. This material is available free of charge via the Internet at http://pubs.acs.org.

References and Notes

(1) Anderson, C. F.; Record, M. T. *Annu. Rev. Phys. Chem.* **1995**, *46*, 657.
(2) Manning, G. S.; Ray, J. *J. Biomol. Struct. Dyn.* **1998**, *16*, 461.
(3) Young, M. A.; Jayaram, B.; Beveridge, D. L. *J. Am. Chem. Soc.* **1997**, *119*, 59.
(4) Strauss, J. K.; Maher, L. J. *Science* **1994**, *266*, 1829.
(5) Williams, L. D.; Maher, L. J. *Annu. Rev. Biophys. Biomol. Struct.* **2000**, *29*, 497.
(6) Bloomfield, V. A. *Biopolymers* **1997**, *44*, 269.
(7) Rouzina, I.; Bloomfield, V. A. *Biophys. J.* **1998**, *74*, 3152.
(8) Hud, N. V.; Plavec, J. *Biopolymers* **2003**, *69*, 144.
(9) Brauns, E. B.; Madaras, M. L.; Coleman, R. S.; Murphy, C. J.; Berg, M. A. *J. Am. Chem. Soc.* **1999**, *121*, 11644.
(10) Brauns, E. B.; Madaras, M. L.; Coleman, R. S.; Murphy, C. J.; Berg, M. A. *Phys. Rev. Lett.* **2002**, *88*, 158101.
(11) Somoza, M. I.; Andreatta, D.; Coleman, R. S.; Murphy, C. J.; Berg, M. A. *Nucleic Acids Res.* **2004**, *32*, 2495.
(12) Sen, S.; Paraggio, N. A.; Gearheart, L. A.; Connor, E. E.; Issa, A.; Coleman, R. S.; Wilson, D. M., III.; Wyatt, M. D.; Berg, M. A. *Biophys. J.* **2005**, *89*, 4129.
(13) Andreatta, D.; Pérez Lustres, J. L.; Kovalenko, S. A.; Ernsting, N. P.; Murphy, C. J.; Coleman, R. S.; Berg, M. A. *J. Am. Chem. Soc.* **2005**, *127*, 7270.
(14) Andreatta, D.; Sen, S.; Pérez Lustres, J. L.; Kovalenko, S. A.; Ernsting, N. P.; Murphy, C. J.; Coleman, R. S.; Berg, M. A. *J. Am. Chem. Soc.* **2006**, *128*, 6885.
(15) Pal, S. K.; Zhao, L. A.; Zewail, A. H. *Proc. Natl. Acad. Sci. U.S.A.* **2003**, *100*, 8113.
(16) Pal, S. K.; Zhao, L.; Xia, T.; Zewail, A. H. *Proc. Natl. Acad. Sci. U.S.A.* **2003**, *100*, 13746.
(17) Coleman, R. S.; Madaras, M. L. *J. Org. Chem.* **1998**, *63*, 5700.
(18) Maroncelli, M.; Fleming, G. R. *J. Chem. Phys.* **1987**, *86*, 6221.
(19) Moog, R. S.; Davis, W. W.; Ostrowski, S. G.; Wilson, G. L. *Chem. Phys. Lett.* **1999**, *299*, 265.
(20) Sen, S.; Andreatta, D.; Ponomarev, S. Y.; Beveridge, D. L.; Berg, M. A. *Phys. Rev. Lett.*, submitted for publication.
(21) Hynes, J. T. *Theory of Chemical Reactions*; CRC Press: Boca Raton, FL, 1985; Vol. 4.
(22) Jimenez, R.; Fleming, G. R.; Kumar, P. V.; Maroncelli, M. *Nature* **1994**, *369*, 471.
(23) Várnai, P.; Zakrzewska, K. *Nucleic Acids Res.* **2004**, *32*, 4269.
(24) Ponomarev, S. Y.; Thayer, K. M.; Beveridge, D. L. *Proc. Natl. Acad. Sci. U.S.A.* **2004**, *101*, 14771.
(25) Chapman, C. F.; Maroncelli, M. *J. Phys. Chem.* **1991**, *95*, 9095.
(26) Anderson, C. F.; Record, M. T. *Annu. Rev. Biophys. Biophys. Chem.* **1990**, *19*, 423.
(27) Bleam, M. L.; Anderson, C. F.; Record, M. T. *Proc. Natl. Acad. Sci. U.S.A.* **1980**, *77*, 3085.
(28) Marincola, F. C.; Denisov, V. P.; Halle, B. *J. Am. Chem. Soc.* **2004**, *126*, 6739.
(29) Denisov, V. P.; Halle, B. *Proc. Natl. Acad. Sci. U.S.A.* **2000**, *97*, 629.
(30) McConnell, K. J.; Beveridge, D. L. *J. Mol. Biol.* **2000**, *304*, 803.
(31) Cheatham, T. E.; Kollman, P. A. *Annu. Rev. Phys. Chem.* **2000**, *51*, 435.
(32) Lyubartsev, A. P.; Laaksonen, A. *J. Biomol. Struct. Dyn.* **1998**, *16*, 579.
(33) Takeshita, M.; Chang, C. N.; Johnson, F.; Will, S.; Grollman, A. P. *J. Biol. Chem.* **1987**, *262*, 10171.
(34) Crespo-Hernández, C. E.; Cohen, B.; Hare, P. M.; Kohler, B. *Chem. Rev.* **2004**, *104*, 1977.
(35) Velapoldi, R. A.; Mielenz, K. D. *Standard Reference Materials: A Fluorescence Standard Reference Material: Quinine Sulfate Dihydrate*; U.S. Government Printing Office, Washington, DC, 1980.
(36) Melhuish, W. H. *J. Res. Natl. Bur. Stand., Sect. A* **1972**, *76*, 547.
(37) O'Connor, D. V. *Time Correlated Single Photon Counting*; Academic Press: London, 1984.
(38) Birch, D. S.; Imhof, R. E. Time-Domain Fluorescence Spectroscopy Using Time-Correlated Single-Photon Counting. In *Topics in Fluorescence Spectroscopy: Techniques*; Lakowicz, J. R., Ed.; Plenum Press: New York, 1991; Vol. 1, p 1.
(39) Ma, J.; Fourkas, J. T.; Vanden Bout, D. A.; Berg, M. A. Multiple Time Scales in the Nonpolar Solvation Dynamics of Supercooled Liquids. In *Supercooled Liquids: Advances and Novel Applications*; Fourkas, J. T., Kivelson, D., Mohanty, U., Nelson, K. A., Eds.; ACS Symposium Series 676; American Chemical Society: Washington, DC, 1997; p 199.
(40) Fourkas, J. T.; Berg, M. A. *J. Chem. Phys.* **1993**, *98*, 7773.
(41) Stratt, R. M. *Acc. Chem. Res.* **1995**, *28*, 201.
(42) *Lange's Handbook of Chemistry*, 15th ed.; Dean, J. A., Ed.; McGraw-Hill: New York, 1999.
(43) Zwanzig, R. *Nonequilibrium Statistical Mechanics*; Oxford University Press: New York, 2001.
(44) Mukamel, S. *Principles of Nonlinear Optical Spectroscopy*; Oxford University Press: New York, 1995.
(45) Richert, R. *J. Chem. Phys.* **2001**, *114*, 7471.
(46) Gearheart, L.; Somoza, M. M.; Rivers, W. E.; Murphy, C. J.; Coleman, R. S.; Berg, M. A. *J. Am. Chem. Soc.* **2003**, *125*, 11812.
(47) Paulsen, M. D.; Anderson, C. F.; Record, M. T., Jr. *Biopolymers* **1988**, *27*, 1249.
(48) Tereshko, V.; Minasov, G.; Egli, M. *J. Am. Chem. Soc.* **1999**, *121*, 3590.
(49) Maroncelli, M.; Fleming, G. R. *J. Chem. Phys.* **1988**, *89*, 5044.
(50) Hagerman, P. J. *Annu. Rev. Biophys. Biophys. Chem.* **1988**, *17*, 265.
(51) Baumann, C. G.; Smith, S. B.; Bloomfield, V. A.; Bustamante, C. *Proc. Natl. Acad. Sci. U.S.A.* **1997**, *94*, 6185.
(52) Barnett, R. N.; Cleveland, C. L.; Joy, A.; Landman, U.; Schuster, G. B. *Science* **2001**, *294*, 567.